Preparation of Nanoscale UV Filter

Punthita Inthakuntee

Patsita Suphansomboon

A Report Submitted in Partial Fulfillment of the Requirements

for the Degree of Bachelor of Engineering (Petrochemical Engineering)

Department of Chemical Engineering, School of Engineering,

King Mongkut's Institute of Technology Ladkrabang

Academic Year 2022

This material is reserved for educational use only, not allowed for commercial use.

Forbidden to modify the content, and cite the document when use

การสังเคราะห์ตัวกรองรังสียูวีระดับนาโน

ปัญญ์ฑิตา อินทขันตี

พัชญ์สิตา สุพรรณสมบูรณ์

ปริญญานิพนธ์นี้เป็นส่วนหนึ่งของการศึกษาตามหลักสูตรวิศวกรรมศาสตรบัณฑิต

สาขาวิศวกรรมปิโตรเคมี ภาควิชาวิศวกรรมเคมี คณะวิศวกรรมรรมศาสตร์

สถาบันเทคโนโลยีพระจอมเกล้าเจ้าคุณทหารลาดกระบัง

ปีการศึกษา 2565

This material is reserved for educational use only, not allowed for commercial use.
Forbidden to modify the content, and cite the document when use

Title	Preparation of Nanoscale UV Filter
By	Punthita Inthakuntee
	Patsita Suphansomboon
Field of study	Petrochemical Engineering
Advisor	Assoc. Prof. Dr. Teeraporn Suteewong

Accepted by the School of Engineering, King Mongkut's Institute of Technology Ladkrabang in Partial Fulfillment of the Requirements for the Degree of Bachelor of Engineering (Petrochemical Engineering).

Thesis committee

TEERAPORN Chairman

(Assoc. Prof. Dr. Teeraporn Suteewong)

Tanawan Pinnarat Committee

(Asst. Prof. Dr. Tanawan Pinnarat)

T. Samanmulya Committee

(Asst. Prof. Dr. Thachanan Samanmulya)

This material is reserved for educational use only, not allowed for commercial use.
Forbidden to modify the content, and cite the document when use

Title	Preparation of Nanoscale UV Filter
By	Punthita Inthakuntee
	Patsita Suphansomboon
Advisor	Assoc. Prof. Dr. Teeraporn Suteewong
Field of study	Petrochemical Engineering
Affiliation	Department of Chemical Engineering, School of Engineering, King Mongkut's Institute of Technology Ladkrabang

Abstract

Excessive exposure to ultraviolet (UV) radiation has now been found to cause damage and can be life-threatening, such as sunburn, premature aging, eye damage, heat stroke, and plant death. UV filters are used to reduce the intensity of UV, for example, as a component in sunscreen to absorb or block UV rays, or in solar filters for agriculture, etc. In this study, we have developed UV filters with various sizes and structures such as core-shell and hollow structures to develop an effective UV filter, that does not negatively affect the environment. The synthesis involved calcium silicate (Ca_2SiO_4), core-shell of silicon dioxide (SiO_2)-coated zinc oxide (ZnO) (SiO_2@ZnO), and hollow ZnO nanoparticles. The Ca_2SiO_4 particles synthesized effectively protected against UVC but were not suitable for further study. Synthesis of SiO_2@ZnO nanoparticles was investigated by studying the effects of solvent, core size of SiO_2, and concentration of ZnO precursor. The SiO_2@ZnO particles were then evaluated for their optical properties and UV protection efficiency. The appropriate conditions were selected for etching the SiO_2 core using sodium hydroxide at different time intervals to obtain hollow ZnO nanoparticles. The optical property of SiO_2@ZnO and hollow ZnO nanoparticles suggest that both particles can block UVA and can be used as UV filters.

Keywords: UV filter, Sunscreen, Zinc oxide, Hollow ZnO nanoparticles

This material is reserved for educational use only, not allowed for commercial use.
Forbidden to modify the content and cite the document when use

เรื่อง	การสังเคราะห์ตัวกรองรังสียูวีระดับนาโน
โดย	ปัญญ์ทิตา อินทขันตี
	พัชญ์สิตา สุพรรณสมบูรณ์
อาจารย์ที่ปรึกษา	รศ.ดร.ธีรพร สุธีวงศ์
สาขาวิชา	วิศวกรรมปิโตรเคมี
สังกัด	ภาควิชาวิศวกรรมเคมี คณะวิศวกรรมศาสตร์
	สถาบันเทคโนโลยีพระจอมเกล้าเจ้าคุณทหารลาดกระบัง

บทคัดย่อ

ในปัจจุบันพบว่าการได้รับรังสีอัลตราไวโอเลต (Ultraviolet; UV) ที่มากเกินไปทำให้เกิดความเสียหายและอาจเป็นอันตรายต่อชีวิต เช่น ผิวหนังไหม้ แก่ก่อนวัย ทำลายดวงตา เกิด heat stroke และทำให้พืชตายได้ เป็นต้น ตัวกรองรังสี UV (UV filter) ถูกนำมาใช้ในการลดทอนความเข้มของ UV เช่น เป็นส่วนประกอบในครีมกันแดดเพื่อดูดซับหรือป้องกันแสง UV หรืออยู่ในฟิลม์กรองแสงสำหรับทางการเกษตร เป็นต้น ในงานวิจัยนี้ทำการพัฒนาตัวกรองรังสี UV ที่มีขนาดและโครงสร้างต่างๆ เช่น แบบแกน-เปลือก และแบบกลวง เพื่อพัฒนาตัวกรองแสง UV ที่มีประสิทธิภาพและไม่ส่งผลเสียต่อสิ่งแวดล้อม โดยทำการสังเคราะห์อนุภาคแคลเซียมซิลิเกต (Ca_2SiO_4) อนุภาคแบบแกน-เปลือกของซิลิกอนไดออกไซด์ (SiO_2)-ถูกเคลือบด้วยซิงค์ออกไซด์ (ZnO) (SiO_2@ZnO) และอนุภาคแบบกลวงของ ZnO ระดับนาโนสเกล ผลการศึกษาพบว่าอนุภาค Ca_2SiO_4 ที่สังเคราะห์สามารถป้องกันรังสีในช่วงยูวีซี (UVC) จึงไม่นำมาศึกษาต่อ และสังเคราะห์ SiO_2@ZnO โดยศึกษาผลของตัวทำละลาย ขนาดอนุภาคของแก่น SiO_2 และความเข้มข้นของสารตั้งต้น ZnO อนุภาคแบบกลวงของ SiO_2@ZnO ถูกนำมาตรวจสอบคุณสมบัติทางแสงและคำนวณประสิทธิภาพในการป้องกันแสงยูวีเพื่อเลือกสภาวะที่เหมาะสม และนำอนุภาคของ SiO_2@ZnO มากัดด้วยโซเดียมไฮดรอกไซด์ที่เวลาต่างๆ เพื่อทำให้ได้อนุภาคแบบกลวงของ ZnO สมบัติทางแสงของอนุภาคแบบแกน-เปลือกของ SiO_2@ZnO และอนุภาคแบบกลวงของ ZnO แสดงว่าอนุภาคทั้งสองสามารถป้องกันรังสียูวีเอและนำมาใช้เป็นตัวกรองรังสียูวีได้

คำสำคัญ: ตัวกรองรังสีอัลตราไวโอเลต, ครีมกันแดด, ซิงค์ออกไซด์, อนุภาคซิงค์ออกไซด์แบบกลวง

This material is reserved for educational use only, not allowed for commercial use.
Forbidden to modify the content, and cite the document when use

Acknowledgements

We would like to take this opportunity to express our gratitude to Assoc. Prof. Dr. Teeraporn Suteewong, the advisor gave advice, knowledge, and advice in all aspects and corrected any shortcomings. Doing the project on the topic of the Preparation of hollow silica nanoparticles as UV filter resulted in the successful completion of this thesis.

Secondly, I would like to thank our senior, who gave the advice during the process of completing the thesis and provided useful information for us, thus contributing to the success of this thesis.

Next, I would like to thank Asst. Prof. Dr. Tanawan Pinnarat and Asst. Prof. Dr. Thachanan Samanmulya as well as all chemical engineering program teachers for their knowl edge, Suggestions and recommendations throughout the study.

Finally, we would like to thank our parents and friends very much for their encouragement. Help and support throughout the year.

Punthita Inthakuntee
Patsita Suphansomboon

This material is reserved for educational use only, not allowed for commercial use.
Forbidden to modify the content, and cite the document when use

Table of Contents

Page

This material is reserved for educational use only, not allowed for commercial use.
Forbidden to modify the content and cite the document when use

This material is reserved for educational use only, not allowed for commercial use.
Forbidden to modify the content and cite the document when use

List of Figures

Page

This material is reserved for educational use only, not allowed for commercial use.

Forbidden to modify the content and cite the document when use

List of Tables

Page

This material is reserved for educational use only, not allowed for commercial use.
Forbidden to modify the content and cite the document when use

Nomenclature

Abbreviation Title	Full Title
$CePO_4$	Cerium orthophosphate
Ca_2SiO_4	Calcium silicate
$CaCO_3$	Calcium carbonate
CTAB	Cetyl trimethyl ammonium bromide
$C_4H_8O_2$	Ethyl acetate
C_2H_5OH	Ethanol
CeO_2	Cerium dioxide
$Ca(NO_3)_2$	Calcium nitrate
h-SiO_2 NPs	Hollow silica-nanoparticles
IL	Ionic liquid
MgO	Magnesium oxide
MCX	Octal methoxycinnamate
MCX-MS	Mesoporous silicon-dioxide
NH_4OH	Ammonium hydroxide
NH_3	Ammonia
NaOH	Sodium hydroxide
NPs	Nanoparticles
ROS	Reactive oxygen species
SiO_2	Silicon dioxide or Silica
TEM	Transmission Electron Microscope
TiO_2	Titanium dioxide
TEOS	Tetraethyl orthosilicate
TEP	Triethyl phosphaste
UV	Ultraviolet
UVR	Ultraviolet radiation
UV-A	Ultraviolet A

This material is reserved for educational use only, not allowed for commercial use.
Forbidden to modify the content, and cite the document when use

UV-B	Ultraviolet B
UV-C	Ultraviolet C
ZnO	Zinc oxide

This material is reserved for educational use only, not allowed for commercial use.
Forbidden to modify the content, and cite the document when use

CHAPTER I

INTRODUCTION

1.1 Background

Titanium dioxide (TiO_2), and zinc oxide (ZnO) are widely used as ultraviolet (UV) filter. The UV filter is divided into two types, according to the mode of action: physical and chemical UV filters [1]. Scattering and absorption of the physical or inorganic UV filter have the advantage over the chemical or organic UV filter in broader spectrum protection (covering both UVA and UVB) [2], while the chemical or organic UV filter has only absorption and conformational molecular changes [3],[4]. The UV filter has been used in the field of cosmetics, pharmaceuticals, wastewater treatment, and self-cleaning coatings for windows, etc.

As UV filters, TiO_2 and ZnO are often synthesized in the form of nanoparticles (NPs) [5]. Both TiO_2 and ZnO are semiconductor with a wide band gap, which could have the disadvantage to the environment, including bioaccumulation, and the formation of reactive oxygen species (ROS). ZnO causes sea urchin anomalies due to Zn^{2+} emissions, coral bleaching, and shrimp mortality [6]. They photocatalytically degrade organic constituents upon UV exposure and cause skin damage [7]. A lot of research have been tried to find a physical UV filter to replace TiO_2 and ZnO. Mitchnick et al. (1999) [8] analyzed the photodegradation of silica (SiO_2) coated and uncoated ZnO and TiO_2 NPs. The results show that both TiO_2 and ZnO coated with the SiO_2 have a higher photocatalytic level than the uncoated TiO_2 and ZnO. Rafid et al. (2022) [9] synthesized sodium (Na)-doped ZnO NPs with spherical morphology and particle size of 64.6-84.6 nm for photocatalytic comparison. The results showed that the

This material is reserved for educational use only, not allowed for commercial use.
Forbidden to modify the content, and cite the document when use

photocatalytic activity of Na-doped ZnO produced by sol-gel method was reduced by 98%, which was greater than that of the solvothermal method. The band gap in UVA region was increased with an increasing amount of Na-doped during the UVA region.

Thus, the target of this work is to synthesize calcium silicate (Ca_2SiO_4) and hollow ZnO as UV filters at the nanoscale, which can reduce photocatalytic activity while still effectively block UVR. Ca_2SiO_4 serves as an inorganic UV filter with the advantage of low photocatalytic activity [10]. In a part of ZnO is attractive as a UV filter due to its advantageous properties, such as a high refractive index (1.7) and minimal absorption of solar radiation in the UV range, specifically at or below 385 nm. However, it has the disadvantage of high photocatalytic activity [11]. To remedy this disadvantage, the synthesis of ZnO in a hollow morphology is desired. This will be achieved by etching core-shell particles of SiO_2-coated ZnO (SiO_2@ZnO) using sodium hydroxide (NaOH). All the particles will be analyzed for their UV absorption using UV-vis spectrophotometer. The morphology and particle size will be examined using Transmission Electron Microscopy (TEM) and Dynamic Light Scattering (DLS), respectively. The functional groups and the crystallinity of the particles will be analyzed using Fourier Transform Infrared (FTIR) spectroscopy and X-ray Diffraction (XRD), respectively.

1.2 Objectives

1.2.1 To synthesize and characterize of Ca_2SiO_4, SiO_2@ZnO and hollow ZnO NPs.

1.2.2 To study the effect of particle size of NPs prepared in 1.2.1 on the ability to block UV.

This material is reserved for educational use only, not allowed for commercial use.
Forbidden to modify the content, and cite the document when use

1.3 Scopes of Work

1.3.1 Synthesis of Ca_2SiO_4 NPs

1.3.2 Syntheses of SiO_2 NPs at three different sizes.

1.3.3 Syntheses of SiO_2@ZnO and hollow ZnO.

- Vary core size and concentration of ZnO precursor
- Vary etching times

1.3.4 Characterization of Ca_2SiO_4, SiO_2@ZnO and hollow ZnO NPs

- UV-vis Spectrophotometer
- Transmission Electron Microscope (TEM)
- Dynamic Light Scattering (DLS)
- Fourier Transform Infrared (FTIR)
- X-Ray Diffraction (XRD)

1.4 Expected Output

1.4.1 Synthesis protocols of Ca_2SiO_4 NPs.

1.4.2 Syntheses protocols of core-shell SiO_2@ZnO and hollow ZnO.

This material is reserved for educational use only, not allowed for commercial use.
Forbidden to modify the content, and cite the document when use

CHAPTER II

LITERATURE REVIEW

2.1 Ultraviolet radiation (UV)

Ultraviolet radiation (UV) is defined as that portion of electromagnetic radiation lies between X-rays and visible light depending on wavelength as follow [12]:

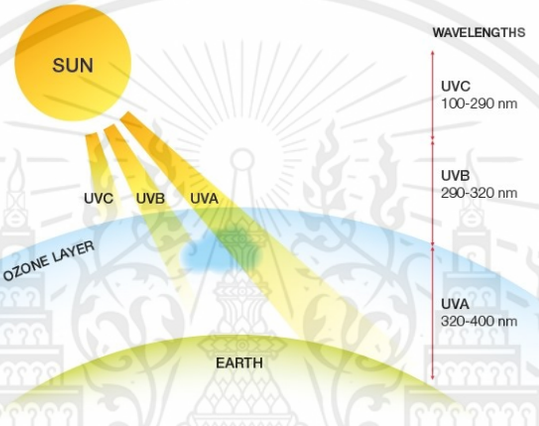

Figure 1 UV in various ranges as follows:

Ultraviolet A (UV-A): It has a radiation range of 320 to 400 nm. It causes skin coloring, due to the excessive production of melanin in the outer layer of the skin.

Ultraviolet B (UV-B): It has a radiation range of 290 to 320 nm. UV-B is also 1000 times more potent and more genotoxic than UV-A.

Ultraviolet C (UV-C): It has a radiation range of 100 to 290 nm. UV-C radiation is in the stratospheric ozone layer. It may cause eye injury and severe skin burns. It is important to avoid direct skin contact with UV-C rays and to not look at the UV-C light source. It may cause the risk of skin cancer and permanent vision loss.

This material is reserved for educational use only, not allowed for commercial use.
Forbidden to modify the content, and cite the document when use

2.2 Evaluation of UV screening efficiency

The ability of UV filter can be specified in many ways, such as UV-shielding performance, percentage of blocking and Sun Protection Factor (SPF).

2.2.1 UV-shielding performance [12]

The Ultraviolet Protection Factor (UPF) value is used to estimate how much the material reduces UV exposure. It can be calculated as **Equation 1.** The standard grades of UPF and its classification were shown in **Table 1**.

$$UPF = \frac{\int_{280}^{400} E(\lambda)S(\lambda)d\lambda}{\int_{280}^{400} E(\lambda)S(\lambda)T(\lambda)d\lambda} \quad (1)$$

Where;

λ = Wavelength (nm)

E(λ) = The relative erythema action spectrum

S(λ) = The spectral irradiance (Wm^{-2}/nm)

T(λ) = Average spectral transmittance

dλ = The wavelength interval between measurements (nm)

Table 1 Standard grades of UPF and its classification.

UPF rating	% of UV blocking	UV protection category
15-24	93-96%	Good
25-39	96-97%	Very good
40-50+	97-99%	Excellent

This material is reserved for educational use only, not allowed for commercial use.
Forbidden to modify the content, and cite the document when use

2.2.2 The percentage of blocking

The percentage UVR block relates to the performance of the reflect or absorb incident UV within 290 nm to 400 nm. This includes UV-A radiation and UV-B radiation.

$$UV - A\ blocking(\%) = 100\ - \frac{\int_{320}^{400} T(\lambda)d\lambda}{\int_{320}^{400} d\lambda}(\%) \qquad (2)$$

$$UV - B\ blocking(\%) = 100\ - \frac{\int_{280}^{320} T(\lambda)d\lambda}{\int_{280}^{320} d\lambda}(\%) \qquad (3)$$

2.2.3 Determination of SPF

All the sunscreens available in the market have different SPF values depending upon the protection intensity against UV radiation. SPF value is basically the ratio of minimal erythemal dose on the sunscreen protected skin to the minimal erythemal dose on the unprotected skin [13].

$$SPF = \frac{Minimal\ erythemal\ dose\ on\ sunscreen\ protected\ skin}{Minimal\ erytthernal\ dose\ on\ unproteted\ skin} \qquad (4)$$

SPF values can also be determined by UV-vis spectrophotometry using Mansur mathematical equation. The constant values used for the calculation can be found in **Table 2.**

$$SPF\ spectrophotometric = CF\ x \sum_{290}^{320} EE(\lambda)\ x\ I(\lambda) x\ Abs\ (\lambda) \qquad (5)$$

Where;

This material is reserved for educational use only, not allowed for commercial use.
Forbidden to modify the content, and cite the document when use

CF is correction factor (=10)

EE (λ) is erythemal effect spectrum

I (λ) is solar intensity spectrum

Abs (λ) is absorbance of sunscreen product

Table 2 Values for calculating SPF.

Wavelength (nm)	EE*I
290	0.0150
295	0.0817
300	0.2874
305	0.3278
310	0.1864
315	0.0837
320	0.0180

2.3 UV filters

UV filters are materials that can partially absorb or block UV radiation. UV filters are regularly used in cosmetics for sun protection purposes and can be classified into two groups according to their physicochemical properties, namely chemical UV filters (organic UV filters) and physical UV filters (inorganic UV filters) [2].

2.3.1 Classification of UV filters and mode of action

UV filters into chemical UV filters (organic UV filters) and physical UV filters (inorganic UV filters). There are several modes of UV filtrations, depending on chemical structure/composition, size, component, and morphology.

This material is reserved for educational use only, not allowed for commercial use.
Forbidden to modify the content, and cite the document when use

2.3.1.1 Chemical UV filters (organic UV filters)

Chemical or organic UV filters are usually aromatic compounds with a carbonyl group that absorb UVR to prevent it from reaching the skin. Examples of chemical UV filters are avobenzone, cinoxate, encapsule, oxybenzone, etc.

Chemical UV filters can function in 3 ways from **Figure 2**. The first is to undergo conformational molecular changes Later, high-wavelength radiation was emitted, and the incident energy was released as heat [3],[4]. The action mode of organic is reversible so that the same molecule can work repeatedly. In addition, the absorption of UV photons by organic UV filters can release free radicals and cause damage to collagen and elastin [14]. Therefore, the use of organic UV filters is often questioned due to their side effects.

2.3.1.2 Physical UV filters (inorganic UV filters)

Physical or inorganic UV filters are generally metallic oxides, principally working by reflecting, scattering, and absorbing UV radiation from **Figure 2.** Also, they can protect against visible light, UVB, and UVA rays. These substances include titanium dioxide (TiO_2), zinc oxide (ZnO), calcium carbonate ($CaCO_3$), calcium silicate (Ca_2SiO_4), kaolin, talc, magnesium oxide (MgO), etc [1]. It consists of reflection which depends on refractive index (*n*), scatter which depends on scattering efficiency and absorption, which often relates to photocatalytic.

This material is reserved for educational use only, not allowed for commercial use.
Forbidden to modify the content, and cite the document when use

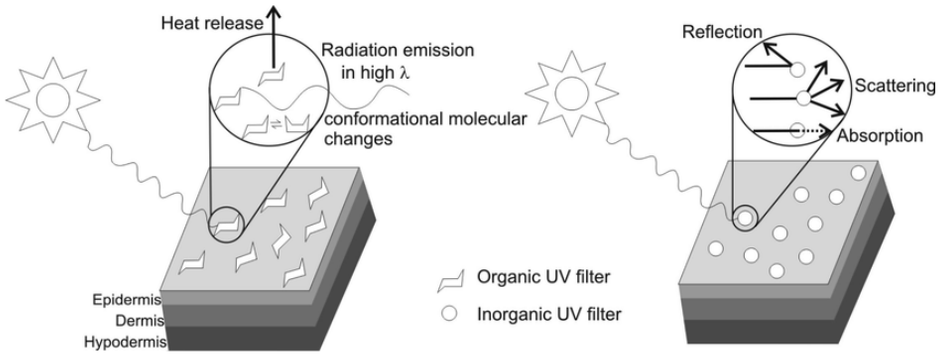

Figure 2 Action mode of organic and inorganic UV filters.

A. Refractive index (n) refers to the ratio between the speed of an electromagnetic wave in a vacuum and its speed in another medium.

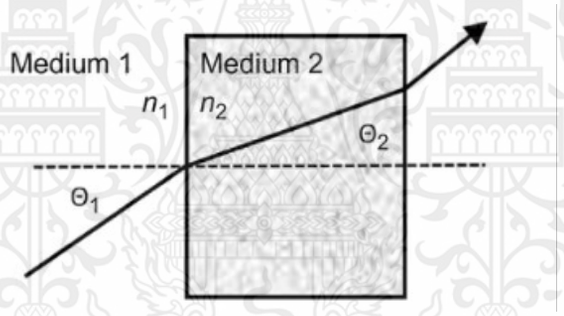

Figure 3 Light bends at the interface of two mediums.

Snell's Law index of refraction could be calculated as

$$\frac{n_1}{n_2} = \frac{\sin\theta_1}{\sin\theta_2} \qquad (6)$$

Where; n_1 and n_2 are refractive indices of medium 1 and 2, θ_1 is the angle of incidence, θ_2 is the angle of refraction, respectively.

The refractive index of a medium can be calculated using the following formula:

This material is reserved for educational use only, not allowed for commercial use.
Forbidden to modify the content, and cite the document when use

$$n = c/v = C/f\lambda \quad (7)$$

Where;

n is the refractive index of the medium

c is the velocity of light in a vacuum (m/s)

v is the velocity of light in the medium (m/s)

λ is the wavelength of light (m)

f is the frequency of light (s^{-1})

Table 3 Examples of refractive index

Chemical	Refractive index
TiO_2	2.7
ZnO	1.7
CeO_2	1.9
Ca_2SiO_4	1.6
SiO_2	1.5

B. Scattering is the mechanism through which light is transmitted in all directions when it strikes a particle with a larger diameter and intensity of scattered light is a function of the wavelength of the light ray. The scattering efficiency is given by the Rayleigh Equation.

$$q_{sca} = \frac{C}{V} = \frac{K.V}{\lambda^4} \quad (8)$$

Where;

This material is reserved for educational use only, not allowed for commercial use.
Forbidden to modify the content, and cite the document when use

q_{sca} is the scattering efficiency

C is the scattering cross-section (m^2)

K is a constant whose size is a function of m, the ratio of the refractive index of the particle

V is the particle volume (m^3)

λ is the wavelength of the incident light in the medium (m)

C. The Tyndall effect (Tyndall scattering) is the scattering of light by colloidal (size). For a mixture to be a colloid, the particles must be in the range of 1-1000 nm in diameter. The size of the scattering particles determines the color of the scattered light and colloidal particles absorb energy from incoming light [2] and difference between Tyndall effect and scattering of light is that the scattering of light is the spread of light in all directions by the particles that are present in its path.

D. A band gap is the distance between the valence band of electrons and the conduction band. Importantly, the band gap represents the minimum energy that is required to excite an electron up to a state in the conduction band where it can participate in conduction.

The band gap energy can be obtained from the formula:

$$\text{Band gap energy } (E) = hc/\lambda \quad (9)$$

This material is reserved for educational use only, not allowed for commercial use.
Forbidden to modify the content, and cite the document when use

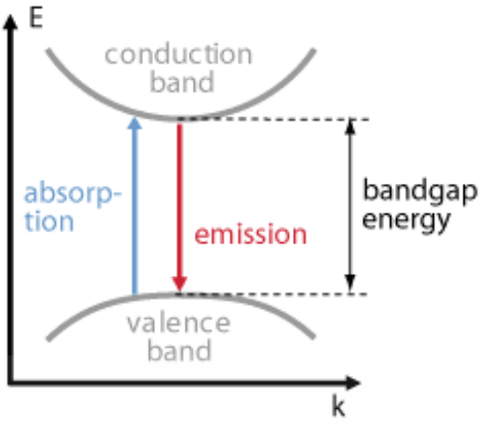

Figure 4 Direct band gap

Where;

E is the band gap energy (eV)

h is the planks constant = 6.626 x 10^{-34} J.S

c is the speed of light = 3.0 x 10^{8} m/s

λ is the cut-off wavelength (m)

2.4 Literature review

2.4.1 Calcium silicate nanoparticles (Ca_2SiO_4)

CS is inorganic UV filters characterized by low photocatalytic activity. It leaves an amount of white residue on the skin. It also has a low refractive index of 1.6. It is highly stable for the skin and has a high SPF. It was found that Ca_2SiO_4 shows the maximum absorbance in range UVB along with covering the entire UV region from 290 to 385 nm. Also, XRD and FTIR confirmed the good crystallinity and no chemical interaction among the components. So, it aims to produce better quality and effective sunscreen [10].

This material is reserved for educational use only, not allowed for commercial use.
Forbidden to modify the content, and cite the document when use

2.4.2 Silica nanoparticles (SiO_2 NPs)

SiO_2 NPs are the most common materials found in the Earth's crust. It has been observed that SiO_2 acts as a chemically stable shell as it cannot absorb light in the visible region and poses no toxicological threat [13]. There are three main types of SiO_2: (1) crystalline SiO_2 and (2) amorphous SiO_2 (Naturally occurring or by-product in the form of fused silica or fume silica) and (3) synthetic amorphous SiO_2 [15]. There are various morphologies of SiO_2 NPs such as nonporous, mesoporous, hollow, core- shell, yolk-shell or Janus [16].

The most widely used method to synthesize SiO_2 NPs is the sol-gel method, a chemical method used for the synthesis of various nanostructures, especially oxide nanoparticles. This method is performed at low temperatures (usually below 100ºC) and in the liquid state, in which two reactions occur: hydrolysis and condensation, starting with the formation of a homogeneous solution between the precursor and the solvent (usually water, alcohol and organic solvent). The hydrolysis reaction between water and a precursor occurs in which water breaks down a complex compound into a simple compound and allows SiO_2 NPs to come together to form solid particles dispersed in the solvent. Those SiO_2 NPs that are fine dispersed in the solvent phase is called the sol formation. The next step is a condensation reaction, that has the final product is an oxide network Si-O-Si consisting of a SiO_2 NPs group. A condensation reaction is that the simple molecules join together (two hydroxides or one hydroxide (Si-OR) + one metal alkoxide (HO-Si)) resulting in -OH and -H is released as water from **Figure 5.**

This material is reserved for educational use only, not allowed for commercial use.
Forbidden to modify the content, and cite the document when use

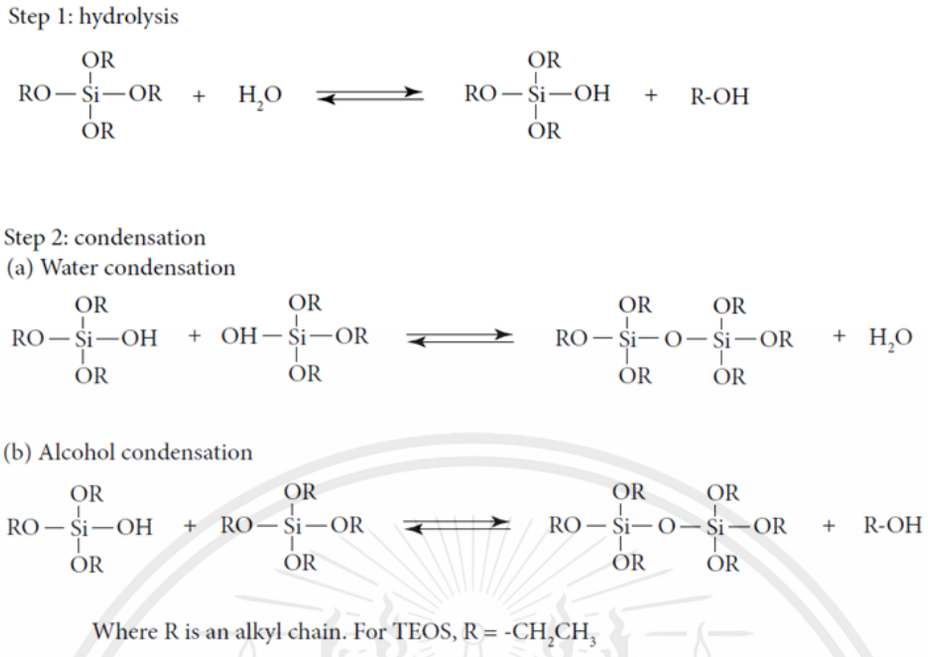

Figure 5 Hydrolysis reaction and condensation of water and alcohol [18].

2.4.3 SiO_2 nanoparticles as UV filter

Zhang et al. (2014) [17] synthesized two types of SiO_2 NPs with a hollow core and dense spherical structure at the same particle size of ~ 50 nm, and used pig skin as a model instead of human skin. It was found that hollow nanoparticles have less penetrating ability than SiO_2 nanosphere with a dense structure, making them safer for the skin because of a high UV-attenuating efficiency and SPF.

Chen-Yang et al. (2011) [18] studied UV filter octal methoxycinnamate (MCX) encapsulated in mesoporous SiO_2 (MCX-MS), prepared by sol-gel method using TEOS as precursor with ionic liquid (IL) as solvent and pore-forming agent. MCX was used as an additive. According to the comparison between free MCX and MCX-MS, it was found that the SPF of MCX-MS increased from free MCX by 57%. Moreover, the average particle size of MCX-

This material is reserved for educational use only, not allowed for commercial use.
Forbidden to modify the content, and cite the document when use

MS emulsion droplets was large enough to prevent skin penetration damage. Because the MCX particles are larger than 10 nm, they can prevent skin penetration [19]. As for the UV absorption of SiO_2 samples, it can be found that the UV absorption of MS is higher than dense SiO_2 (nonporous) because much higher SPF values of MS (12.6) than that of MCX (8.0) indicates a synergistic enhancement in the UV protection ability, which can be determined from the reflection and scattering of light in the mesopores of MS. The presence of MCX encapsulated by MS increases the UV absorption capacity between 290-400 nm due to the presence of MCX, confirming that significant amount of the MCX molecules was encapsulated in the mesoporous SiO_2 matrix.

Gallardo et al. (2010) [20] report a new class of sunscreens called progressive sunscreens. It is based on compounds such as pre-avobenzone, pre-diethylamino hydroxy benzoyl hexyl benzoate, and pre-OXY that undergo a chemical change upon exposure to sunlight and produce avobenzone, diethylamino hydroxy benzoyl hexyl benzoate and OXY, respectively. This was done to improve the phototransformation yield and photostability to avoid the release of the UV filter into the environment. The UV filter was encapsulated in SiO_2 by a copolymerization method using the precursor silil 3-(3-triethoxysilyl) propoxyphenyl benzoate (precursor of the OXY UV filter) in the sol–gel method.

2.4.4 Zinc oxide (ZnO) nanoparticles

ZnO is an inorganic compound that is often used as the main component of sunscreen products. ZnO is composed of two crystalline wurtzite and zinc-blend, see **Figure 6**. It was found that wurtzite is preferred over Zinc-Blend due

This material is reserved for educational use only, not allowed for commercial use.
Forbidden to modify the content, and cite the document when use

to its greater stability. ZnO provides effective protection against UVA rays through reflection and scattering. The properties of ZnO are low production cost, availability, and non-toxicity. It also has the wide band gap of 3.37 eV, good optical transparency, high electron mobility, photostability, and controllable shape and size. There are various factors, such as precursor concentrations, duration, temperature, surfactant concentration, solvent medium, and dopant. Concentration and pH of the reaction mixture, and source of light during synthesis affecting the shape, size, and optical properties of ZnO [21].

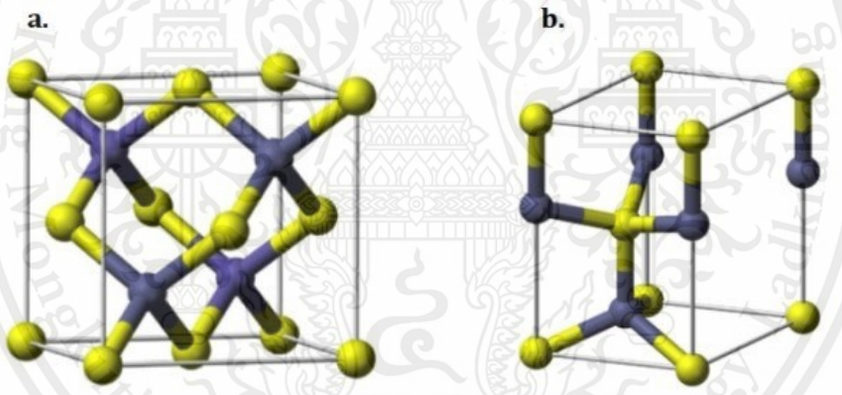

Figure 6 (a) Zinc-blend and (b) wurtzite type structures.

The sol-gel method is the simplest and cost-effectiveness route to synthesize of nanoparticles. The sol-gel method also controls the composition easily [22]. During this process, the mixture containing the reactant and the surfactant was stirred on a magnetic stirrer until a gel was formed. The resulting white precipitate was removed by centrifugation.

This material is reserved for educational use only, not allowed for commercial use.
Forbidden to modify the content, and cite the document when use

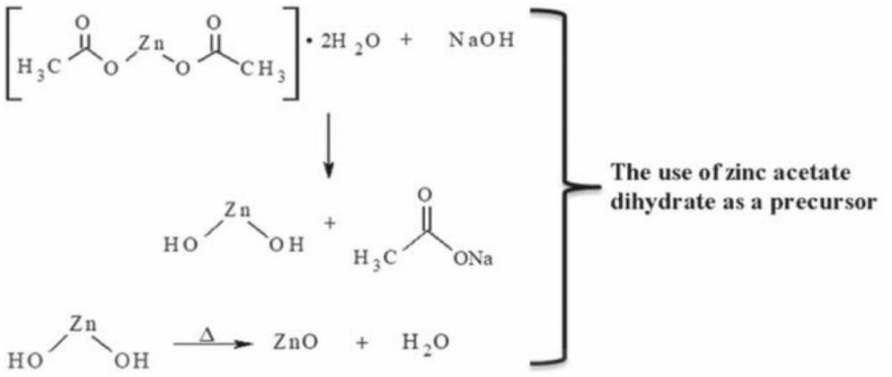

Figure 7 Hydrolysis and condensation reactions of acetate dihydrate for ZnO.

2.4.5 ZnO nanoparticles as UV filter

Zhenxiang et al. (2020) [23] synthesized Na-doped ZnO nanoparticles by the sol-gel technique to reduce their photocatalytic activity. The particle size was around 64.6-84.6 nm. It was found that particle size decreased as a function of doping concentration. UV-visible results of Na-doped ZnO NPs showed less absorption compared to undoped commercial ZnO but they exhibited less degradation compared with commercial ZnO regarding the dye. Na-doped ZnO NPs samples have a polycrystalline structure and very good crystallinity.

This material is reserved for educational use only, not allowed for commercial use.
Forbidden to modify the content, and cite the document when use

CHAPTER III

RESEARCH METHODOLOGY

3.1 Materials

The chemicals used in this research are tetraethoxysilane (TEOS), ammonium hydroxide (NH_4OH), ethanol (C_2H_6O), sodium hydroxide (NaOH), zinc acetate dihydrate ($Zn(CH_3CO_2)_2 \cdot 2H_2O$), cetyltrimethylammonium bromide (CTAB), and calcium nitratetetrahydrate ($Ca(NO_3)_2 \cdot 4H_2O$)

3.2 Methods

3.2.1 Syntheses of calcium silicate nanoparticles (CS NPs) with CTAB addition (CS_CT) and without CTAB addition (CS_NCT)

CS NPs were prepared by adding CTAB (0.004 g) and DI water (10.37 mL). Then add NH_4OH 0.2664 mL to the CTAB solution as the catalyst and stir for 1 hr at room temperature. Next, add TEOS (0.034 mL) and $Ca(NO_3)_2 \cdot 4\ H_2O$ (0.067 g) and vigorously stir for 3 hr at room temperature. Remove the excess chemicals by centrifugation at the speed of 10,000 rpm for 10 minutes. Similar manner was also performed in the absence of CTAB.

3.2.2 Syntheses of dense silica nanoparticles (SiO_2 NPs) sample 1 (size 450.9 nm)

SiO_2 NPs was prepared by the sol-gel method using TEOS as silica precursor in a basic ethanol medium. Starting by mixing 38.15 mL of ethanol and 2.32 mL of NH_4OH for 10 minutes. Then add 1.317 mL of TEOS into the prepared solution and stir for 1 hr. Then add 17 µl of TEOS into the mixture

This material is reserved for educational use only, not allowed for commercial use.
Forbidden to modify the content, and cite the document when use

every 5 minutes for 10 times and stir for 8 hr. Then remove the excess chemicals by centrifugation at the speed of 10,000 rpm for 10 minutes.

3.2.3 Syntheses of dense silica nanoparticles (SiO_2 NPs) sample 2, 3, 4 and 5.

Syntheses of SiO_2 NPs were varied in a concentration of TEOS (sample 4 and 5) and NH_4OH (sample 2 and 3). The first step was to add ethanol and NH_4OH to the round bottom flask but only sample 5 add DI water and stir for 10 min then add TEOS were stirred for 1 h at room temperature, then dropwise of TEOS into the mixture and stir, after which centrifuged several times with ethanol and water was to obtain SiO_2 NPs.

3.2.4 Syntheses of core-shell SiO_2@ZnO NPs

The synthesis of ZnO nanoparticles coated on SiO_2 starts by mixing SiO_2 particles with three concentrations of zinc acetate: 0.019 M, 0.032 M, and 0.097 M, which serves as the precursor for ZnO. The mixture is stirred at a temperature of 60ºC for 5 minutes. Then, a solution of NaOH in ethanol with a concentration of 0.25 M is added to the mixture. The mixture is continuously stirred for 4 hr to allow the reaction to take place. Afterward, the particles are washed with water and ethanol to remove any residual chemicals. In the case of varying the core size of SiO_2, the same synthesis method as varying the concentration of zinc acetate can be used. However, the concentration of zinc acetate will be fixed at 0.097 M.

This material is reserved for educational use only, not allowed for commercial use.
Forbidden to modify the content, and cite the document when use

3.2.5 Syntheses of hollow ZnO NPs

The synthesis of hollow ZnO starts by adding 0.25 M NaOH (1 mL) to DI water (24.918 mL), followed by stirring for 10 minutes at room temperature. Then, the SiO_2@ZnO (1.061 g) in DI water are added to the mixture for etching at three different times: 15 min, 1 hr and 3 hr. At each time interval, a 10 mL sample is washed with water and ethanol.

3.2.6 Determination of UV absorption by UV-vis spectrophotometer

A UV-vis spectrophotometer (EvolutionTM 201/220, Thermo Scientific) will be used to measure the absorption of samples. The mass concentration used for measuring is 0.2 mg/ml (0.2 mg with particles dispersed in ethanol). The absorption spectra of sample in the solution were measured at 5 nm intervals in the wavelength of 200 to 700 nm. Scan speed is 300 nm/min.

3.2.7 Characterization by Transmission Electron Microscope (TEM)

The morphology of SiO_2, SiO_2@ZnO and hollow ZnO NPs can be observed by TEM (JEOL 2100 Plus). Particles size and size distributions of SiO_2 and SiO_2@ZnO NPs were measured by ImageJ program.

3.2.8 Characterization by Dynamic Light Scattering (DLS)

Hydrodynamic size and size distributions of SiO_2 and SiO_2@ZnO NPs in ethanol were measured by DLS (MALVERN Zetasizer Nano ZSP).

This material is reserved for educational use only, not allowed for commercial use.
Forbidden to modify the content, and cite the document when use

3.2.9 Characterization by Fourier transform infrared spectroscopy (FTIR)

The functional groups of samples were measured by FTIR (Spectrum Two FT-IR Spectrometer, PerkinElmer Scientific), from wave number of 400 to 4000 cm^{-1}.

3.2.10 Characterization by X-ray diffraction (XRD)

The crystallinity can be measured using X-ray diffraction (XRD) (Rigaku Smartlab), where the sample is dried at 60°C for 8 hours to obtain a solid powder form.

This material is reserved for educational use only, not allowed for commercial use.
Forbidden to modify the content, and cite the document when use

CHAPTER IV

RESULTS AND DISCUSSION

We were interested in three types of particle UV filters: Ca_2SiO_4 NPs, SiO_2@ZnO NPs and hollow ZnO NPs.

4.1 Syntheses of Ca_2SiO_4

4.1.1 Effect of surfactant concentration on UV absorbance

Cetyl trimethyl ammonium bromide (CTAB), a common surfactant used in the synthesis of Ca_2SiO_4 particles, has an effect on particle absorbance. The presence of CTAB 0.2 M increases the excitation energy increases which decreases the absorbance. [24]. From **Figure 8**, it was found that the absorbance of substance containing with CTAB was lower than that of substances without CTAB. From the result in **Figure 8**, the λ_{max} value is 220 nm, which is in the UVC range while other studies on Ca_2SiO_4 particle as UV filter show the λ_{max} in the UVB range. So, this Ca_2SiO_4 was not selected for study.

This material is reserved for educational use only, not allowed for commercial use.
Forbidden to modify the content, and cite the document when use

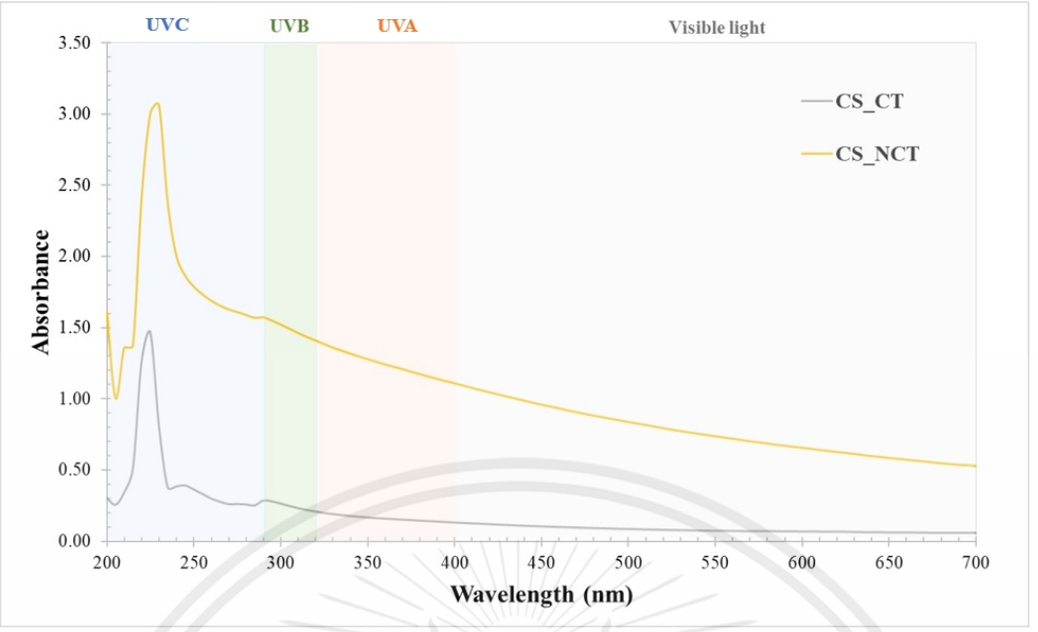

Figure 8 UV-visible spectrum of Ca_2SiO_4 nanoparticles in EtOH.

4.2. Syntheses of SiO_2@ZnO NPs

4.2.1 Effect of TEOS and NH_4OH on the particle size of SiO_2 NPs and absorbance

To vary the particle size, we first varied the concentration of TEOS as seen in **Table 4**. At [NH_4OH] = 0.29 M, when increasing the concentration of TEOS from 0.15 M to 0.23 M, the particle size measured from DLS increased from 153.0 nm to 235.6 nm because TEOS can have an effect on the resulting particle size. Increasing concentration of TEOS can enhance the rate of hydrolysis and condensation reactions. So, higher nucleation and growth rate lead to the formation of larger particles [25].

Next, we further control particle size by varying concentration of NH_4OH from 0.29 to 0.38 M at [TEOS] = 0.15 M. NH_4OH is often used as a catalyst or pH adjuster in the synthesis of dense SiO_2 particles and has an effect on the particle size. From **Table 4**, increasing NH_4OH from 0.29 M in sample

This material is reserved for educational use only, not allowed for commercial use.
Forbidden to modify the content, and cite the document when use

2 to 0.38 M in sample 3 increase the particle size from 153.0 nm to 234.9 nm, respectively. Increasing the NH_4OH leads to larger particle sizes because NH_4OH can increase the pH of the reaction mixture, which can lead to a higher rate of silica particle formation and growth. This higher rate of particle formation and growth can lead to fewer nucleation sites and larger particles [26].

Table 4 $SiO_2$with different concentrations of TEOS and NH_4OH

Sample	Concentration of TEOS (mol/L, M)	Concentration of NH_4OH (mol/L, M)	Particle size (nm)*
1	0.13	0.29	450.9
2	0.15	0.29	153.0
3	0.15	0.38	234.9
4	0.18	0.29	150.9
5	0.23	0.29	235.6

*Number average particle size determined by dynamic light scattering (DLS) technique.

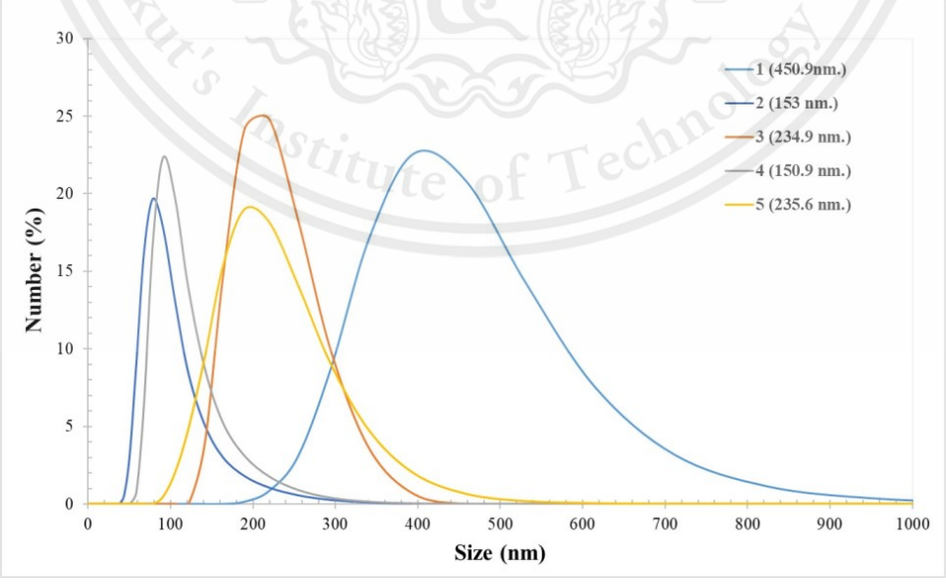

Figure 8 Particle size of SiO_2 prepared from different concentrations of TEOS and NH_4OH.

This material is reserved for educational use only, not allowed for commercial use.
Forbidden to modify the content, and cite the document when use

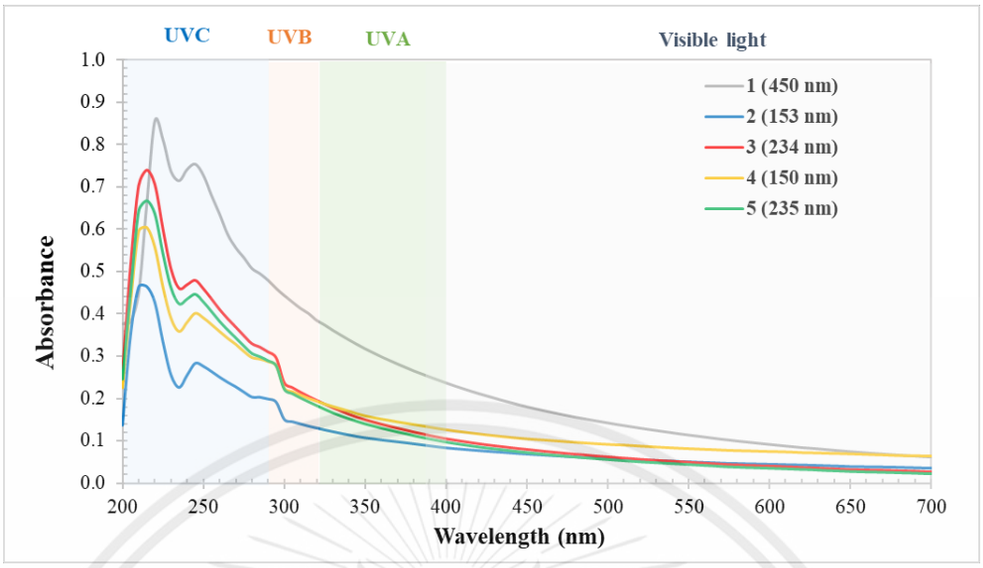

Figure 9 UV-visible spectra of SiO_2 nanoparticles.

From the UV-visible spectrum in **Figure 9**, sample 1 with the largest particle size has the highest absorbance. It can be seen that if the size is larger, it will result in higher absorbance [29], because the peak absorbance increases with particle diameter. It absorbs in the wavelength range of 200-250 nm, which is consistent with the research [29].

4.2.2 Effect of solvents on morphology of SiO_2@ZnO NPs

Ethanol has been chosen as the solvent for the synthesis of SiO_2@ZnO NPs. Two types of ethanol were used for the study: absolute ethanol (purity ≥ 99.9%) and antiseptic ethanol (purity ≥ 95%). The main difference between the two types lies in the water content present in ethanol. Size of SiO_2 core was approximately 150±1 nm (according to number distribution using the DLS method). The synthesis is carried out using a zinc acetate concentration of 0.097 M under the same conditions. The morphology of resulting SiO_2@ZnO NPs was observed using TEM, as shown in **Figure 10**. It can be observed that when

This material is reserved for educational use only, not allowed for commercial use.
Forbidden to modify the content, and cite the document when use

antiseptic ethanol was used as the solvent, disk-like ZnO particles were formed, and did not coat on SiO_2. While ZnO NPs synthesized using absolute ethanol (purity ≥ 99.9%) have coated on SiO_2@ZnO NPs. This difference can be attributed to the increased amount of water content in the solvent, leading to a change in the morphology of ZnO particles from spherical to disk-like [27]. The polarity of the solvent plays a crucial role in determining the growth characteristics and morphology of the particles. In solvents with higher polarity, growth of ZnO tends to occur along the [001] direction, resulting in disk-like or rod-like morphologies [27]. Due to the synthesis requirements of SiO_2@ZnO NPs, where ZnO needs to be coated onto the surface of SiO_2, absolute ethanol is suitable as a solvent. This is because ZnO can effectively coat the SiO_2 particles.

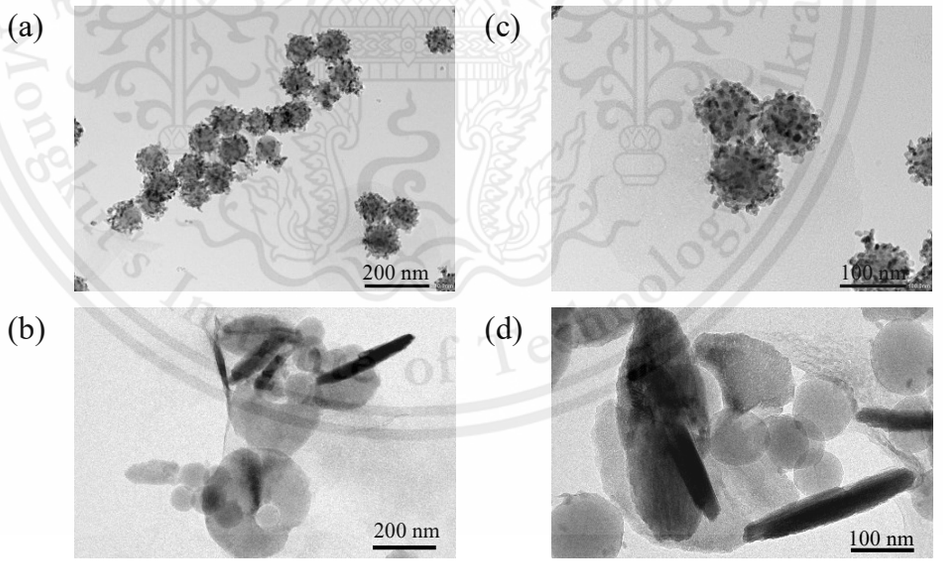

Figure 10 TEM images of SiO_2@ZnO synthesized in: (a, c) absolute ethanol and (b, d) antiseptic ethanol at magnification of 50K (a, b) and 100K (c, d), respectively.

This material is reserved for educational use only, not allowed for commercial use.
Forbidden to modify the content, and cite the document when use

4.2.3 Effect of concentration of zinc acetate

To study the effect of zinc acetate concentration on formation of ZnO NPs on SiO_2, SiO_2 core with 453±5 nm was performed because it has a higher absorbance than other sizes, see **Figure 9**. The concentrations of zinc acetate as a precursor of ZnO were varied from 0.019 M, 0.032 M, and 0.097 M. **Figure 11** showed the morphology of the SiO_2@ZnO NPs, i.e., dense spherical appearance of SiO_2 NPs coated with small spherical ZnO NPs on the surface. The amount of ZnO NPs increased with increasing the concentration of ZnO precursor Zn^{2+} is a positively charged attracted to negatively charged on surface of SiO_2 to form Si-O-Zn bond. At a zinc acetate concentration of 0.019 M, it was observed that the ZnO derived partially attached to the SiO_2 core. At a zinc acetate concentration of 0.032 M, most of the SiO_2 core was coated with ZnO, although the coverage was not uniform. However, at a concentration of zinc acetate equal to 0.097 M, it is found that the quantity of Zn^{2+} ions is sufficient to be attracted to the negatively charged surface of the dense SiO_2 particles throughout the surface. Therefore, it can be concluded that at zinc acetate concentrations of 0.019 M and 0.032 M, the amount of ZnO was insufficient to fully coat to the surface of the SiO_2 core. While the concentration of zinc acetate is 0.097 M, ZnO can fully coat the SiO_2 particles with a size of 453±5 nm. This concentration is considered suitable for the encapsulation of SiO_2 cores.

FITR analysis of SiO_2@ZnO NPs and pure SiO_2 NPs powder were shown in **Figure 12**. The peak of SiO_2@ZnO exhibited a peak at 976.42 cm^{-1}, which was attributed to the bending vibration of Si-OH groups and the symmetric stretching vibration of Si-O-Si in the structure. This peak differed

This material is reserved for educational use only, not allowed for commercial use.
Forbidden to modify the content, and cite the document when use

from pure SiO_2, which showed a peak at 1063.36 cm^{-1}, indicating an asymmetric stretching mode of Si-O-Si. Additionally, a peak at 496.53 cm^{-1} on FTIR spectra indicated the presence of Zn-O vibrations, as well as the emergence of Si-O-Zn vibrations near 660 cm^{-1}, suggesting the formation of covalent bonds between ZnO and SiO_2, possibly indicating the occurrence of a core-shell structure [28].

From **Figure 13**, XRD patterns are shown. SiO_2@ZnO and ZnO NPs (uses the same synthesis method as the synthesis of SiO_2@ZnO) are evident that all of the diffraction peaks at the 2-theta values of 31.3, 34.8, 36.4, 48.2, 57.0, 63.2 and 68.3 index to (100), (002), (101), (102), (110), (103) and (112) were directly indexed to the phase pure hexagonal wurtzite crystalline structure of ZnO. The results indicate the alteration of ZnO crystallinity due to the increasing Zn^{2+} imply more nuclear embryos and faster nucleation rate. Both factors contribute to the crystal growth and increase of crystallinity [28]. The initial synthesis temperature of wurtzite ZnO is typically around 60ºC [29].

This material is reserved for educational use only, not allowed for commercial use.
Forbidden to modify the content, and cite the document when use

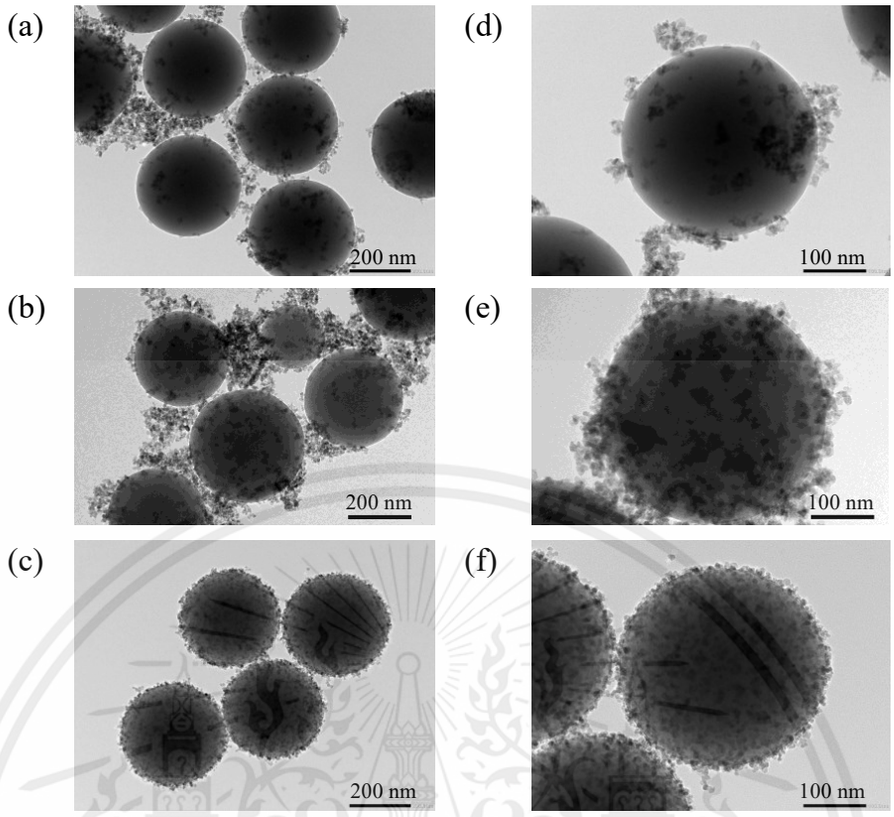

Figure 11 TEM images of SiO_2@ZnO with different concentrations of zinc acetate: (a, d) 0.019 M, (b, e) 0.032 M and (c, f) 0.097 M at magnification of 50K (a, b, c) and 100K (d, e, f), respectively.

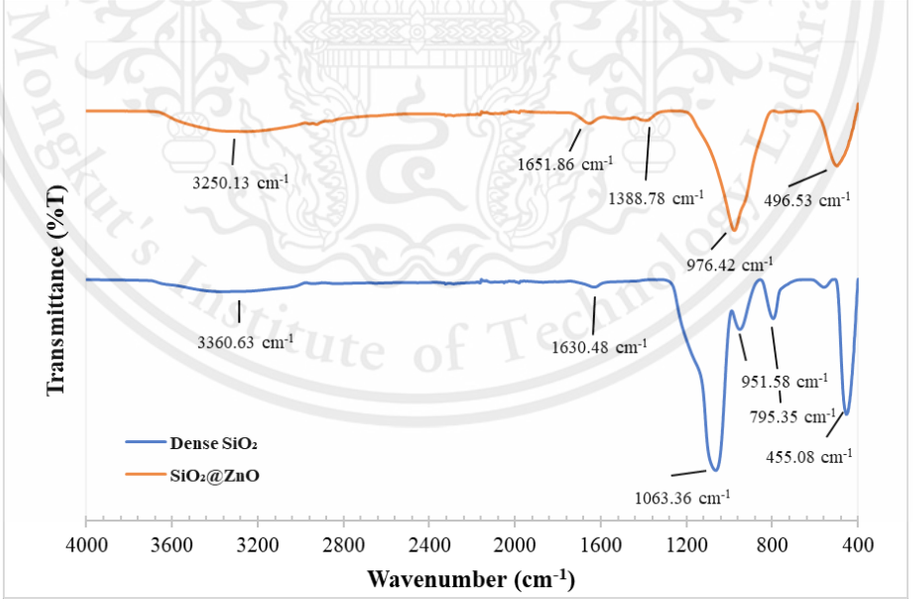

Figure 12 FTIR spectra of SiO_2 and SiO_2@ZnO NPs.

This material is reserved for educational use only, not allowed for commercial use.
Forbidden to modify the content, and cite the document when use

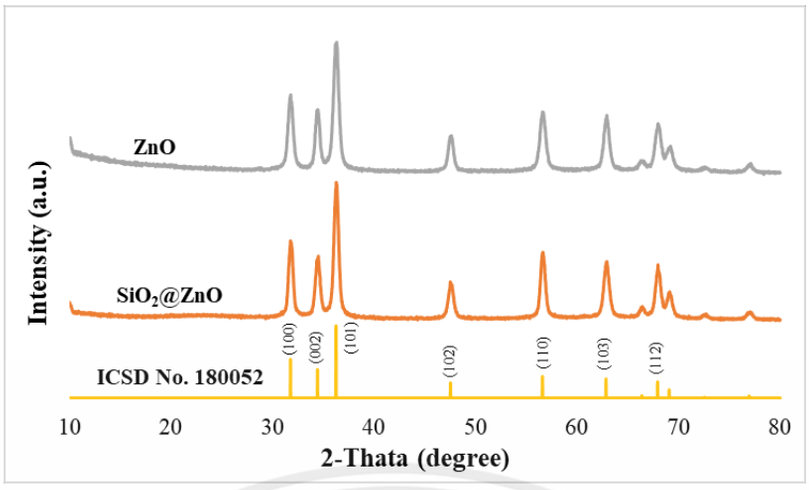

Figure 13 XRD patterns of SiO_2, SiO_2@ZnO and ZnO, reference peaks of ZnO wurtzite (ICSD No. 180052).

The results of SiO_2@ZnO NPs with different concentrations of zinc acetate using SiO_2 with diameter of 453±5 nm as core exhibit UV absorption characteristics as shown in **Figure 14 (a)**. ZnO reveals a peak of UV absorption at a wavelength of 360 nm (UVA range), indicating the characteristic peak of ZnO [30], which differs from the absorbance of dense SiO_2. After coating SiO_2 with ZnO, it is observed that the absorbance values at wavelength 360 nm of all SiO_2@ZnO are higher than that of dense SiO_2, indicating the enhanced efficiency of UV absorption due to the presence of a ZnO. This suggests that coating dense SiO_2 with ZnO enhances the ability to absorb UV radiation, especially UVA region compared to dense SiO_2. Zinc acetate at 0.097 M showed the highest UV absorbance because ZnO can fully coat the SiO_2 nanoparticles.

The SPF values were calculated using Mansur's equation, as described in **Equation 5**, using the absorbance values in the wavelength range of 290-320 nm obtained from the UV absorption spectra shown in **Figure 14 (a)**. The

This material is reserved for educational use only, not allowed for commercial use.
Forbidden to modify the content, and cite the document when use

results of coating dense SiO_2 with varying concentrations of zinc acetate on SPF values are presented in **Figure 14 (b)**, indicating that the concentration of zinc acetate at 0.097 M yield the highest SPF value of 20. On the other hand, the concentrations of zinc acetate at 0.019 M and 0.032 M resulted in the same SPF value, which is 14. These three concentrations fall under the category of very high sun protection (SPF 12-20) as defined by the Food and Drug Administration (FDA). The higher SPF values for the concentrations of 0.097 M of zinc acetate compared to the concentration of 0.019 M and 0.032 M can be attributed to the rough surface of the core-shell nanoparticles, which results in high light scattering properties. **Figure 14 (c)** shows the calculation of UVA/UVB for different concentrations of zinc acetate. It is found that at a zinc acetate concentration of 0.097 M, the UVA/UVB value is the lowest (0.83), indicating that at this concentration, it is more effective in blocking UVB compared to other concentrations. This result is consistent with the UV absorption spectra graph in **Figure 14 (a)**.

This material is reserved for educational use only, not allowed for commercial use.
Forbidden to modify the content, and cite the document when use

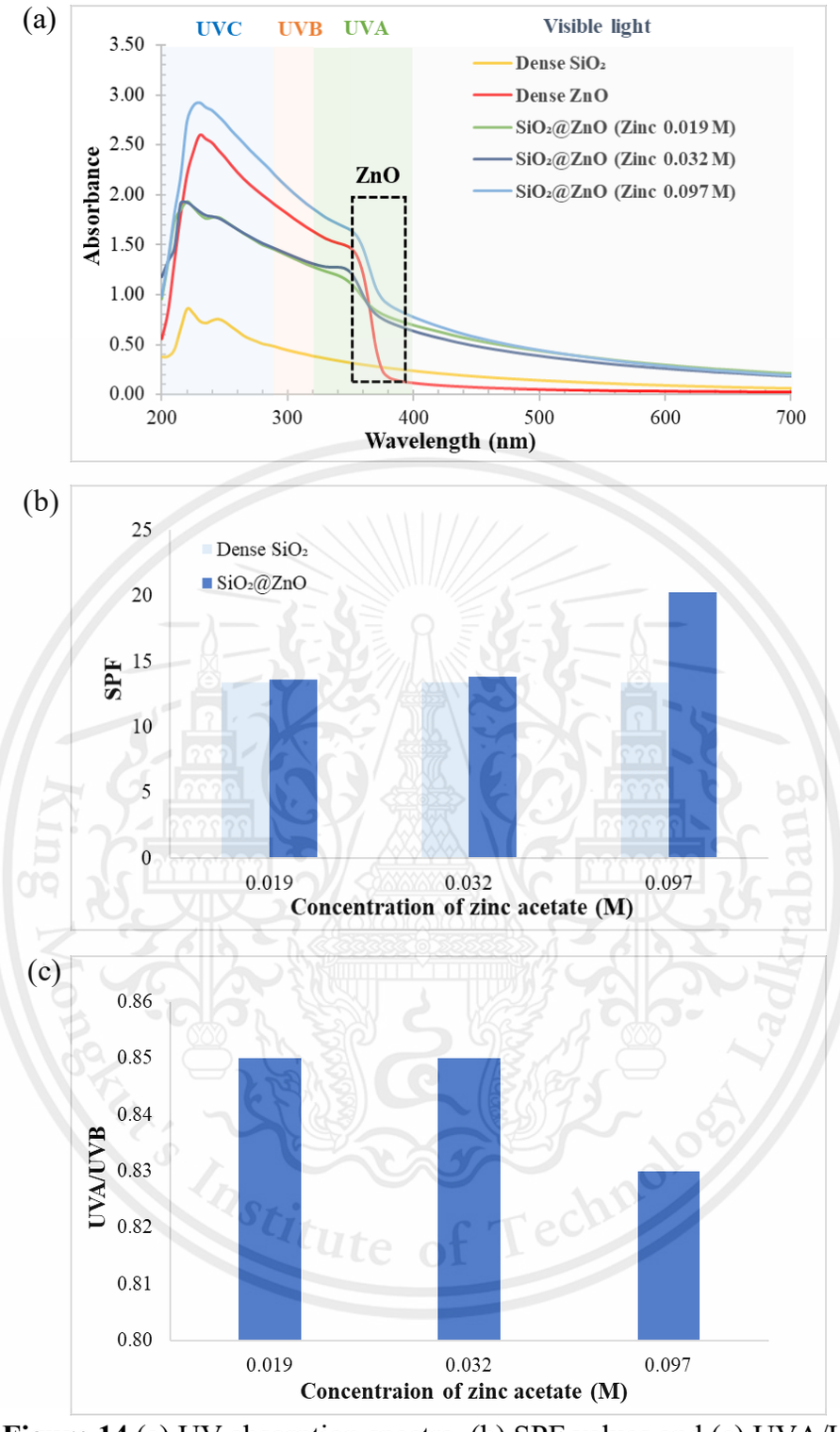

Figure 14 (a) UV absorption spectra, (b) SPF values and (c) UVA/UVB of SiO_2@ZnO NPs prepared from different zinc acetate concentrations.

This material is reserved for educational use only, not allowed for commercial use.
Forbidden to modify the content, and cite the document when use

4.2.4 Effect of core size of SiO_2

To investigate the effect of core sizes, different SiO_2 NPs, i.e., 150±1 nm, 235±4 nm, and 453±5 nm were used to synthesize SiO_2@ZnO at the same zinc acetate concentration (0.097 M). **Figure 15** shows TEM images of all the SiO_2@ZnO composite particles with different SiO_2 core sizes. For the SiO_2 core size of 150±1 nm, the ZnO coating on the SiO_2 particles have covered the entire surface of the SiO_2 particles. Additionally, there were some particle aggregation. At the SiO_2 core size of 235±4 nm, the ZnO NPs coated on the SiO_2 particles have a plate-like shape. This is because a contaminating water during synthesis and greater polar surface area leads to increased activity of the (001) Zn face, which can be attributed to the (001) face of ZnO [23]. As for the SiO_2 core size of 453±5 nm, the ZnO coating on the SiO_2 particles will have the lowest density of ZnO compared to the other two SiO_2 sizes. Therefore, as the size of the SiO_2 core increases, the density of ZnO particles coating the SiO_2 and aggregration decreases. With a constant amount of ZnO precursor, the ratio of Zn^{2+} ions decreases continuously due to the increased particle size of the SiO_2 core. This is because a larger superficial area implies a lower density of functional groups and lower surface energy [28]. The low surface energy of SiO_2 results in less adhesion of ZnO nanoparticles compared to smaller particles with higher surface energy.

The UV absorption results of SiO_2@ZnO NPs with different SiO_2 core sizes at the same concentration of zinc acetate (0.097 M) are shown in **Figure 16 (a)**. It demonstrates that the UV absorption values of SiO_2@ZnO NPs, for all core sizes, are higher than that of dense SiO_2 at the same concentration.

This material is reserved for educational use only, not allowed for commercial use.
Forbidden to modify the content, and cite the document when use

Additionally, SiO_2@ZnO NPs exhibit a peak in UV absorption at a wavelength of 360 nm. This indicates the UV absorption of ZnO NPs. It was found that SiO_2 with 453±5 nm diameter gave the highest UVA absorbtion, which was 2.172 due to the large particle size of SiO_2 NPs, which has low surface energy, it leads to a high particle dispersion of SiO_2@ZnO NPs. There is an increased interaction between ZnO NPs and UVR [28].

The SPF values results of different SiO_2 particle sizes are presented in **Figure 16 (b)**. The SiO_2@ZnO NPs with core size of 453 nm has the highest SPF value, which is 20. The SiO_2@ZnO NPs with core sizes of 150 nm and 235 nm resulted in SPF values of 11 and 16, respectively. The high SPF values are attributed to the rough surface of the core-shell NPs, which results in high light scattering properties. **Figure 16 (c)** shows the calculation of UVA/UVB for different core sizes of SiO_2. It is found that at a SiO_2 core size of 453.9 nm, the UVA/UVB value is the lowest (0.83). This result indicates that at this core size, it is more effective in blocking UVB compared to other core sizes. This result aligns with the UV absorption spectra graph in **Figure 16 (a)**. However, since the UVA/UVB values are very close to each other, the difference is not statistically significant.

This material is reserved for educational use only, not allowed for commercial use.
Forbidden to modify the content, and cite the document when use

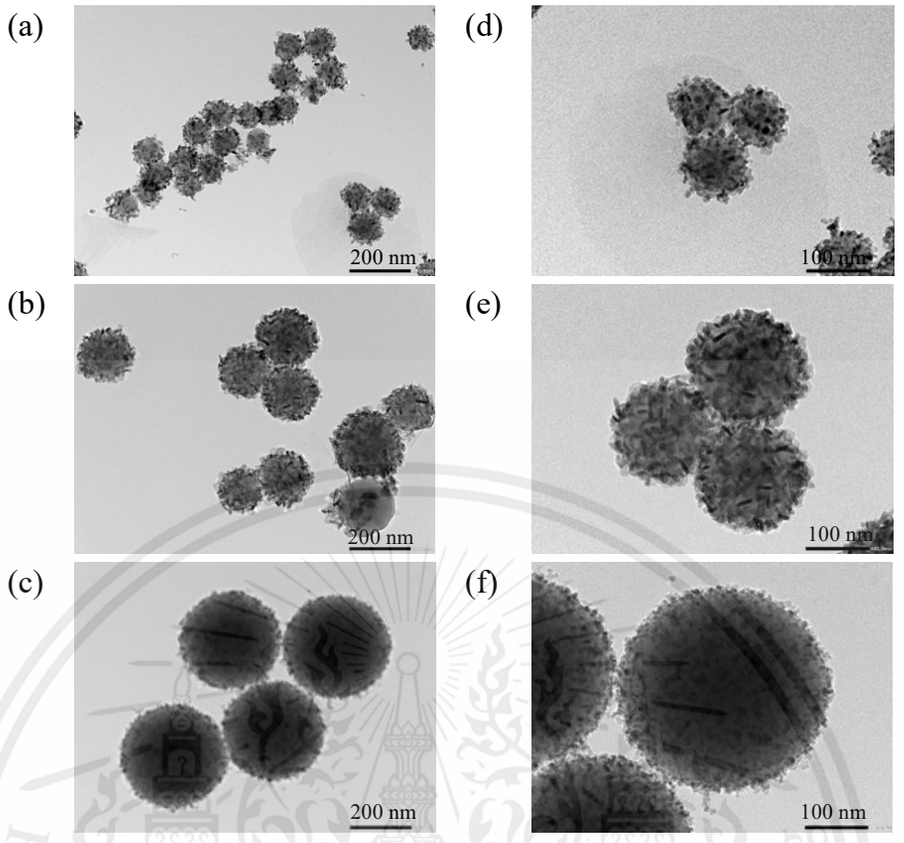

Figure 15 TEM images of SiO_2@ZnO with different SiO_2 core size: (a, d) 150 nm, (b, e) 235 nm and (c, f) 453 nm at magnification of 50K (a, b, c) and 100K (d, e, f), respectively.

This material is reserved for educational use only, not allowed for commercial use.
Forbidden to modify the content, and cite the document when use

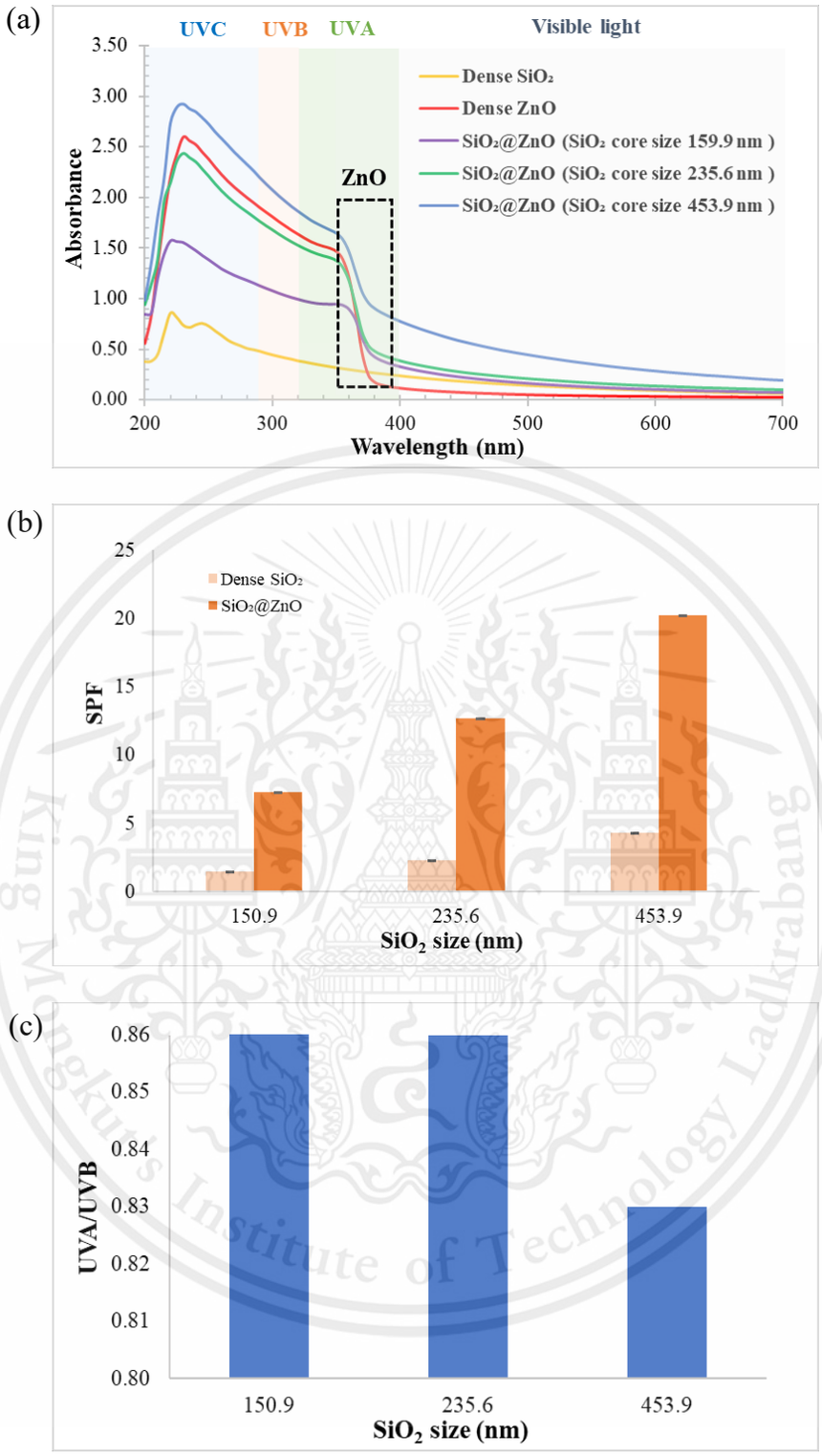

Figure 16 (a) UV absorption spectra, (b) SPF values and (c) UVA/UVB of SiO_2@ZnO NPs with different core sizes of SiO_2.

This material is reserved for educational use only, not allowed for commercial use.
Forbidden to modify the content, and cite the document when use

4.3. Syntheses of hollow ZnO NPs

4.3.1 Effect of etching time

SiO_2@ZnO with a SiO_2 core size of 453±5 nm and a zinc acetate concentration of 0.097 M using NaOH as the etchant were used to study the etching time. Etching times of 15 min, 1 hr, and 3 hr were employed. **Figure 17** showed the morphology of the etched SiO_2@ZnO. It can be observed that at 15 min etching time, the SiO_2 core is completely etched, resulting in the formation of hollow ZnO. However, the resulting hollow ZnO structures exhibited irregular shapes or non-uniform morphology. On the other hand, at etching time at 1 hr and 3 hr, it can be observed that the ZnO particle cracking caused by excessive etching under severe conditions.

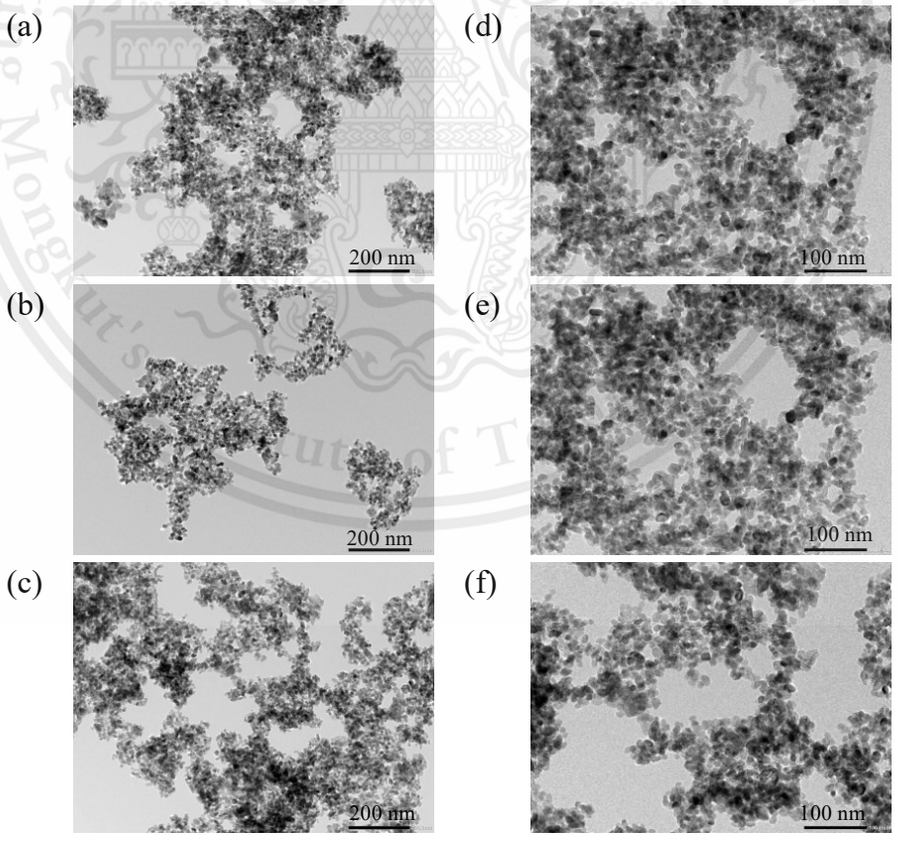

Figure 17 TEM images of hollow ZnO with different etching times: (a, d) 15 min, (b, e) 1 hr. and (c, f) 3 hr. at magnification of 50K (a, b, c) and 100K (d, e, f), respectively.

This material is reserved for educational use only, not allowed for commercial use.
Forbidden to modify the content, and cite the document when use

The UV absorbance of hollow structures with different etching times is shown in **Figure 18 (a)**. It is observed that the highest absorbance occurs at an etching time of 15 minutes compared to the other etching times. Additionally, a prominent peak of ZnO is observed at a wavelength of 360 nm. Looking at the histogram, the absorbance at a wavelength of 360 nm is highest at the etching time of 15 minutes, with a value of 1.701. This is due to the etching time increases, it causes hollow ZnO particles to crack.

Calculating the SPF based on the absorbance values shown in **Figure 18 (b)**, it was found that the etching time of 15 minutes has the highest SPF value of 19, indicating a very high level of sun protection (SPF 12-20) according to FDA standards. The etching times of 1 hr and 3 hrs have SPF values of 11 and 9, respectively, which fall into the category of high sun protection (SPF 8-12) according to FDA standards. Furthermore, when comparing the SPF values before and after etching, it is observed that the SPF value before etching is higher than after etching. This is because the shell of ZnO particles, which loosely adhere and still forms a hollow structure, resulting in an ununiform particle shape and aggregation. That reduces the effectiveness of UV protection.

This material is reserved for educational use only, not allowed for commercial use.
Forbidden to modify the content, and cite the document when use

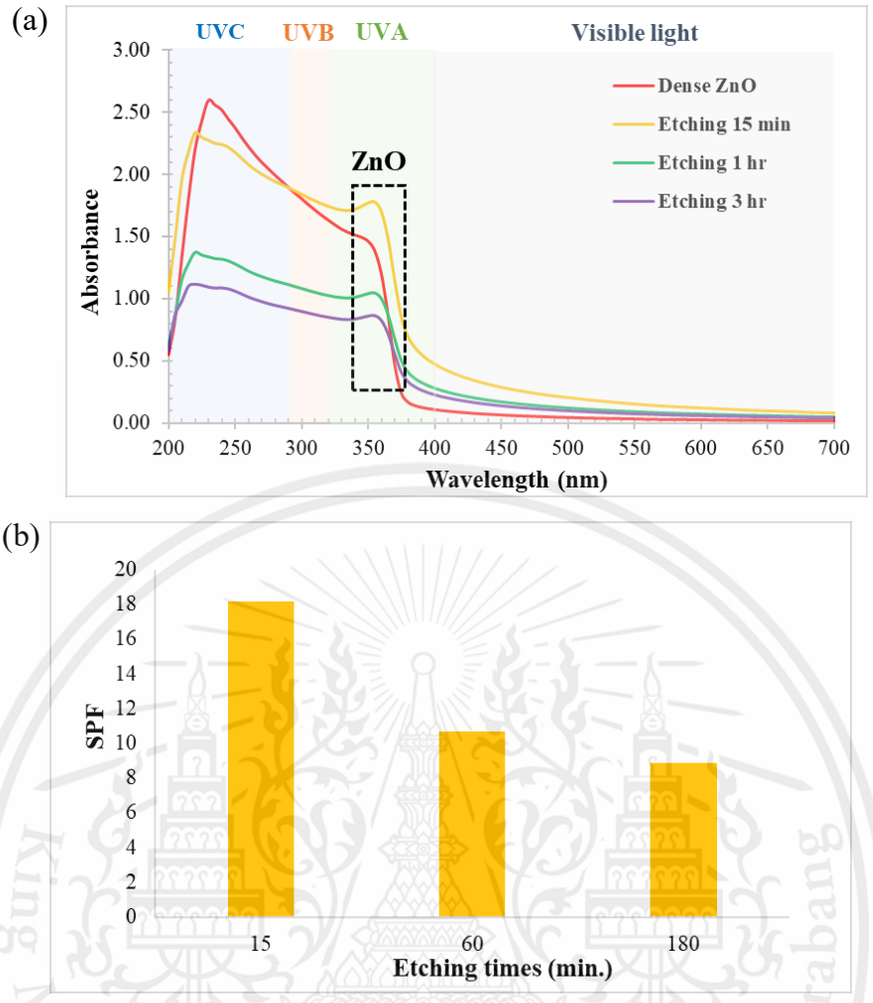

Figure 18 (a) UV absorption spectra and (b) SPF value of hollow ZnO NPs with different etching times.

This material is reserved for educational use only, not allowed for commercial use.
Forbidden to modify the content, and cite the document when use

CHAPTER V

CONCLUSION

In this study, we synthesized SiO_2@ZnO NPs with a core-shell structure using the sol-gel method. We varied the precursor and catalyst, which were TEOS and NH_4OH, respectively. By varying these parameters, we obtained SiO_2 NPs with different particle sizes, specifically 150 nm, 235 nm, and 459 nm. It was found that the particle size of 459 nm had the highest SPF value, which was SPF 13. Subsequently, the dense SiO_2 particles with a size of 459 nm were coated with ZnO using zinc acetate as the precursor of ZnO. It was observed that at a zinc acetate concentration of 0.097 M, the SiO_2 particles were fully coated, and the resulting SiO_2@ZnO NPs shows a high UV absorption at a wavelength of 360 nm. The SPF value for this sample was 20, which was higher than that of the uncoated SiO_2 particles. The same coating process was performed on SiO_2 particles of different sizes using a zinc acetate concentration of 0.097 M. It was found that the SiO_2@ZnO with SiO_2 core of 459 nm still had a higher UV absorption at a wavelength of 360 nm and an SPF value of 20 compared to the other sizes. After determining the suitable core size and zinc acetate concentration, etching with NaOH was conducted at different etching times to obtain hollow ZnO NPs. It was observed that after 15 minutes of etching, the SiO_2 core was completely etched, resulting in hollow ZnO NPs. These hollow ZnO NPs exhibited UV absorption in the UVA range at a wavelength of 360 nm, similar to dense ZnO. Additionally, the SPF value was found to be 19, which was close to that of dense ZnO (SPF 18). From these comprehensive results, it can be concluded that hollow ZnO NPs can serve as UV filters to protect against UVA radiation like dense ZnO, while being environmentally and

This material is reserved for educational use only, not allowed for commercial use.
Forbidden to modify the content, and cite the document when use

human-friendly due to the reduced amount of ZnO through the transformation into a hollow structure.

This material is reserved for educational use only, not allowed for commercial use.
Forbidden to modify the content, and cite the document when use

References

[1] N. J. Lowe, "An overview of ultraviolet radiation, sunscreens, and photo-induced dermatoses," *Dermatologic Clinics*, vol. 24, no. 1. pp. 9–17, Jan. 2006. doi: 10.1016/j.det.2005.08.001.

[2] N. Serpone, D. Dondi, and A. Albini, "Inorganic and organic UV filters: Their role and efficacy in sunscreens and suncare products," *Inorganica Chim Acta*, vol. 360, no. 3, pp. 794– 802, Feb. 2007, doi: 10.1016/j.ica.2005.12.057.

[3] C. Antoniou, M. G. Kosmadaki, A. J. Stratigos, and A. D. Katsambas, "Sunscreens - What's important to know," *J Eur Acad Dermatol Venereol*, vol. 22, no. 9. pp. 1110–1119, Sep. 2008. doi: 10.1111/j.1468-3083.2007.02580.x.

[4] B. Kiss *et al.*, "Investigation of micronized titanium dioxide penetration in human skin xenografts and its effect on cellular functions of human skin-derived cells," *Exp Dermatol*, vol. 17, no. 8, pp. 659–667, Aug. 2008, doi: 10.1111/j.1600-0625.2007.00683.x.

[5] T. G. Smijs and S. Pavel, "Titanium dioxide and zinc oxide nanoparticles in sunscreens: Focus on their safety and effectiveness," *Nanotec Sci Apps*, vol. 4, no. 1. Dove Medical Press Ltd, pp. 95– 112, 2011. doi: 10.2147/nsa.s19419.

[6] M. Abou-Dahech *et al.*, "A mini-review on limitations associated with UV filters," *Arab J Chem*, vol. 15, no. 11. Elsevier B.V., Nov. 01, 2022. doi: 10.1016/j.arabjc.2022.104212.

[7] P. Falcaro, G. Zaccariello, V. Stoyanova, A. Benedetti, and S. Costacurta, "Temperature matters: An infrared spectroscopic investigation on the photocatalytic efficiency of titania coatings," in *Sci Adv Mater*, 7th ed.American Scientific Publishers, 2017, pp. 1330-1337(8).

[8] M. D. F. S. R. P. Mitchnick and D. Fairhurst and S. R. Pinnell, "Microfine zinc oxide (Z-cote) as a photostable UVA/UVB sunblock agent," *J Am Acad Dermatol*, pp. 85–90, Jan. 1999.

[9] R. A. Mueen, M. L. F. Lerch, Z. Cheng, and K. K. Konstantinov, "Na-doped ZnO UV filters with reduced photocatalytic activity for Na-doped ZnO UV filters with reduced photocatalytic activity for sunscreen applications sunscreen applications." [Online]. Available: https://ro.uow.edu.au/aiimpapershttps://ro.uow.edu.au/aiimpapers/3931

[10] N. Abbas *et al.*, "Investigation of calcium silicate as a natural clay-based sunblock: formulation and characterization," *Photodermatol Photoimmunol Photomed*, vol. 37, no. 1, pp. 39–48, Jan. 2021, doi: 10.1111/phpp.12608.

This material is reserved for educational use only, not allowed for commercial use.

Forbidden to modify the content, and cite the document when use

[11] R. Mueen, M. Lerch, Z. Cheng, and K. Konstantinov, "Na-doped ZnO UV filters with reduced photocatalytic activity for sunscreen applications," *J Mater Sci*, vol. 55, no. 7, pp. 2772–2786, Mar. 2020, doi: 10.1007/s10853-019-04122-2.

[12] M. M. Donglikar and S. L. Deore, "Sunscreens: A review," *Pharmacogn J*, vol. 8, no. 3, pp. 171–179, 2016. doi: 10.5530/pj.2016.3.1.

[13] O. P. Egambaram, S. Kesavan Pillai, and S. S. Ray, "Materials science challenges in skin UV protection: A review," *Photochem Photobiol*, vol. 96, no. 4. Blackwell Publishing Inc., pp. 779–797, Jul. 01, 2020. doi: 10.1111/php.13208.

[14] S. K. Jain and N. K. Jain, "Multiparticulate carriers for sun-screening agents," *Int J Cosmet Sci*, vol. 32, no. 2. pp. 89–98, Apr. 2010. doi: 10.1111/j.1468-2494.2010.00547.x.

[15] M. Younes *et al.*, "Re-evaluation of silicon dioxide (E 551) as a food additive," *EFSA J*, vol. 16, no. 1, Jan. 2018, doi: 10.2903/j.efsa.2018.5088.

[16] F. Arriagada, S. Nonell, and J. Morales, "Silica-based nanosystems for therapeutic applications in the skin," *Nanomedicine*, vol. 14, no. 16. Future Medicine Ltd., pp. 2243–2267, Aug. 01, 2019. doi: 10.2217/nnm-2019-0052.

[17] J. Zhang, A. P. Raphael, Y. Yang, A. Popat, T. W. Prow, and C. Yu, "Nanodispersed UV blockers in skin-friendly silica vesicles with superior UV-attenuating efficiency," *J Mater Chem B*, vol. 2, no. 44, pp. 7673–7678, Nov. 2014, doi: 10.1039/c4tb01332h.

[18] Y. W. Chen-Yang *et al.*, "Preparation of UV-filter encapsulated mesoporous silica with high sunscreen ability," *Mater Lett*, vol. 65, no. 6, pp. 1060–1062, Mar. 2011, doi: 10.1016/j.matlet.2010.12.034.

[19] H. Schaefer, J. Lademann, and H. Schaefer, "The role of follicular penetration a differential view," 2001. [Online]. Available: https://karger.com/spp/article-abstract/14/Suppl.%201/23/383414/The-Role-of-Follicular-PenetrationA-Differential?redirectedFrom=fulltext

[20] A. Gallardo *et al.*, "Dose-dependent progressive sunscreens. a new strategy for photoprotection," *Photochem Photobiol Sci*, vol. 9, no. 4, pp. 530–534, 2010, doi: 10.1039/b9pp00188c.

[21] V. Koutu, L. Shastri, and M. M. Malik, "Effect of NaOH concentration on optical properties of zinc oxide nanoparticles," *Mater Sci-Pol*, vol. 34, no. 4, pp. 819–827, Dec. 2016, doi: 10.1515/msp-2016-0119.

[22] B. Manikandan, T. Endo, S. Kaneko, K. R. Murali, and R. John, "Properties of sol-gel synthesized ZnO nanoparticles," *J Mater Sci Mater*

This material is reserved for educational use only, not allowed for commercial use.
Forbidden to modify the content, and cite the document when use

Electron, vol. 29, no. 11, pp. 9474–9485, Jun. 2018, doi: 10.1007/s10854-018-8981-8.

[23] A. Mclaren, T. Valdes-Solis, G. Li, and S. C. Tsang, "Shape and size effects of ZnO nanocrystals on photocatalytic activity," *J Am Chem Soc*, vol. 131, no. 35, pp. 12540–12541, Sep. 2009, doi: 10.1021/ja9052703.

[24] N. A. Asyiqin Anas, Y. W. Fen, N. A. Yusof, N. A. S. Omar, N. S. Md Ramdzan, and W. M. E. M. Mohd Daniyal, "Investigating the properties of cetyltrimethylammonium bromide/ hydroxylated graphene quantum dots thin film for potential optical detection of heavy metal ions," *Materials*, vol. 13, no. 11, Jun. 2020, doi: 10.3390/ma13112591.

[25] Y. Yan, J. Fu, L. Xu, T. Wang, and X. Lu, "Controllable synthesis of SiO_2 nanoparticles: effects of ammonia and tetraethyl orthosilicate concentration," *Micro Nano Lett*, vol. 11, no. 12, pp. 885–889, Dec. 2016, doi: 10.1049/mnl.2016.0434.

[26] I. A. Rahman, P. Vejayakumaran, C. S. Sipaut, J. Ismail, and C. K. Chee, "Size- dependent physicochemical and optical properties of silica nanoparticles," *Mater Chem Phys*, vol. 114, no. 1, pp. 328–332, Mar. 2009, doi: 10.1016/j.matchemphys.2008.09.068.

[27] J. Yin, F. Gao, C. Wei, and Q. Lu, "Water amount dependence on morphologies and properties of ZnO nanostructures in double-solvent system," *Sci Rep*, vol. 4, Jan. 2014, doi: 10.1038/srep03736.

[28] Y. Yang, S. Tan, Y. Cui, G. Fang, Z. Yang, and Y. Li, "Adjustable color and emissivity based on amorphous arrays composed of SiO_2@ZnO," *J Alloys Compd*, vol. 858, Mar. 2021, doi: 10.1016/j.jallcom.2020.158208.

[29] R. Devi Chandra and K. G. Gopchandran, "Simple, low-temperature route to synthesize ZnO nanoparticles and their optical neuromorphic characteristics," *ACS Appl Electron Mater*, vol. 3, no. 9, pp. 3846–3854, Sep. 2021, doi: 10.1021/acsaelm.1c00471.

[30] M. Pudukudy and Z. Yaakob, "Facile synthesis of quasi spherical ZnO nanoparticles with excellent photocatalytic activity," *J Clust Sci*, vol. 26, no. 4, pp. 1187–1201, Jul. 2015, doi: 10.1007/s10876-014-0806-1.

This material is reserved for educational use only, not allowed for commercial use.
Forbidden to modify the content, and cite the document when use

Appendix

This material is reserved for educational use only, not allowed for commercial use.
Forbidden to modify the content, and cite the document when use

Table A-1 Calculate SPF of SiO_2@ZnO NPs at different zinc acetate concentrations.

Wavelength (nm)	CF	(EE*I)	Absorbance			(EE*I)*Abs		
			Zinc acetate (0.019 M)	Zinc acetate (0.032M)	Zinc acetate (0.097 M)	0.019	0.032	0.097
320	10	0.0180	1.278	1.309	1.8657	0.023	0.024	0.034
315	10	0.0837	1.302	1.330	1.9118	0.109	0.111	0.160
310	10	0.1864	1.331	1.354	1.9632	0.248	0.252	0.366
305	10	0.3278	1.360	1.380	2.0170	0.446	0.452	0.661
300	10	0.2874	1.389	1.406	2.0748	0.399	0.404	0.596
295	10	0.0817	1.417	1.432	2.1342	0.116	0.117	0.174
290	10	0.0150	1.447	1.460	2.1977	0.022	0.022	0.033
Sum (EE*I)*Abs						1.362	1.382	2.024
SPF						13.62	13.82	20.24

Table A-2 Calculate SPF of SiO_2@ZnO NPs at different core sizes.

Wavelength (nm)	CF	(EE*I)	Absorbance			(EE*I)*Abs		
			Core size 150.9 nm	Core size 235.6 nm	Core size 453.9 nm	150.9	235.6	453.9
320	10	0.0180	0.994	1.526	1.8657	0.018	0.027	0.034
315	10	0.0837	1.012	1.560	1.9118	0.085	0.131	0.160
310	10	0.1864	1.031	1.596	1.9632	0.192	0.298	0.366
305	10	0.3278	1.053	1.636	2.0170	0.345	0.536	0.661
300	10	0.2874	1.078	1.678	2.0748	0.310	0.482	0.596
295	10	0.0817	1.102	1.719	2.1342	0.090	0.140	0.174
290	10	0.0150	1.127	1.762	2.1977	0.017	0.026	0.033
Sum (EE*I)*Abs						1.057	1.641	2.024
SPF						10.57	16.41	20.24

Table A-3 Calculate the SPF of SiO_2 NPs at different TEOS and NH_4OH.

Wavelength (nm)	CF	(EE*I)	Absorbance					(EE*I)*Abs				
			Dense SiO2	DS_A	DS_B	DS_C	DS_D	Dense SiO2	DS_A	DS_B	DS_C	DS_D
320	10	0.0180	1.294	0.131	0.196	0.1940	0.184	0.023	0.002	0.004	0.003	0.003
315	10	0.0837	1.307	0.135	0.205	0.2006	0.193	0.109	0.011	0.017	0.017	0.016
310	10	0.1864	1.322	0.140	0.215	0.2083	0.202	0.246	0.026	0.040	0.039	0.038
305	10	0.3278	1.338	0.146	0.226	0.2164	0.212	0.439	0.048	0.074	0.071	0.070
300	10	0.2874	1.354	0.151	0.237	0.2246	0.222	0.389	0.043	0.068	0.065	0.064
295	10	0.0817	1.372	0.192	0.296	0.2776	0.278	0.112	0.016	0.024	0.023	0.023
290	10	0.0150	1.392	0.199	0.310	0.2873	0.290	0.021	0.003	0.005	0.004	0.004
Sum (EE*I)*Abs								1.340	0.150	0.232	0.222	0.218
SPF								13.399	1.50	2.32	2.22	2.18

Table A-4 Calculate the SPF of ZnO.

Wavelength (nm)	CF	(EE*I)	Absorbance	(EE*I)*Abs
			ZnO	ZnO
320	10	0.0180	1.636	0.029
315	10	0.0837	1.674	0.140
310	10	0.1864	1.717	0.320
305	10	0.3278	1.760	0.577
300	10	0.2874	1.808	0.519
295	10	0.0817	1.853	0.151
290	10	0.0150	1.899	0.028
Sum (EE*I)*Abs				1.766
SPF				17.66

This material is reserved for educational use only, not allowed for commercial use.
Forbidden to modify the content, and cite the document when use

Table A-5 Calculate the SPF of hollow ZnO at different etching times.

Wavelength (nm)	CF	(EE*I)	Absorbance			(EE*I)*Abs		
			15 min	1 hr	3 hr	15	60	180
320	10	0.0180	1.744	1.026	0.8524	0.031	0.018	0.015
315	10	0.0837	1.765	1.038	0.8622	0.148	0.087	0.072
310	10	0.1864	1.789	1.052	0.8739	0.333	0.196	0.163
305	10	0.3278	1.813	1.067	0.8863	0.594	0.350	0.291
300	10	0.2874	1.841	1.083	0.8993	0.529	0.311	0.258
295	10	0.0817	1.867	1.098	0.9118	0.153	0.090	0.074
290	10	0.0150	1.894	1.114	0.9249	0.028	0.017	0.014
Sum (EE*I)*Abs						1.817	1.069	0.888
SPF						18.17	10.69	8.88

This material is reserved for educational use only, not allowed for commercial use.
Forbidden to modify the content, and cite the document when use